JOURNAL OF BACTERIOLOGY, Oct. 2009, p. 6292–6299 Vol. 191, No. 20
0021-9193/09/$08.00+0 doi:10.1128/JB.00824-09

Organophosphate Hydrolase in *Brevundimonas diminuta* Is Targeted to the Periplasmic Face of the Inner Membrane by the Twin Arginine Translocation Pathway▽

Purushotham Gorla,[1] Jay Prakash Pandey,[1] Sunil Parthasarathy,[1] Mike Merrick,[2] and Dayananda Siddavattam[1]*

Department of Animal Sciences, School of Life Sciences, University of Hyderabad, Hyderabad 500 046, India,[1] and Department of Molecular Microbiology, John Innes Centre, Colney Lane, Norwich NR4 7UH, United Kingdom[2]

Received 24 June 2009/Accepted 10 August 2009

A twin arginine translocation (Tat) motif, involved in transport of folded proteins across the inner membrane, was identified in the signal peptide of the membrane-associated organophosphate hydrolase (OPH) of *Brevundimonas diminuta*. Expression of the precursor form of OPH carrying a C-terminal His tag in an *opd*-negative background and subsequent immunoblotting with anti-His antibodies showed that only the mature form of OPH associated with the membrane and that the precursor form of OPH was entirely found in the cytoplasm. When OPH was expressed without the signal peptide, most of it remained in the cytoplasm, where it was apparently correctly folded and showed activity comparable to that of the membrane-associated OPH encoded by the wild-type *opd* gene. Amino acid substitutions in the invariant arginine residues of the Tat signal peptide affected both the processing and localization of OPH, confirming a critical role for the Tat system in membrane targeting of OPH in *B. diminuta*. The localization of OPH to the periplasmic face of the inner membrane in *B. diminuta* was demonstrated by proteinase K treatment of spheroplasts and also by fluorescence-activated cell sorting analysis of cells expressing OPH-green fluorescent protein fusions with and without an SsrA tag that targets cytoplasmic proteins to the ClpXP protease.

Bacterial organophosphate hydrolases (OPH), also known as phosphotriesterases, have been shown to hydrolyze a structurally diverse group of phosphotriesters used as insecticides and chemical warfare agents (26, 37). The genetic information required to encode these dimeric metalloenzymes is highly conserved and often located on plasmids known as organophosphate-degrading (*opd*) plasmids (27). Among the *opd* plasmids, pPDL2 (40 kb), isolated from *Flavobacterium* sp. strain ATCC27551, and pCMS1 (66 kb), isolated from *Brevundimonas diminuta* (formerly *Pseudomonas diminuta*), are well characterized (27). In these two indigenous plasmids, a 7-kb region that includes the 1.5-kb organophosphate-degrading (*opd*) gene is highly conserved and has the features of a complex transposon (38).

OPH has been crystallized from a number of sources and has been shown to be a dimeric metalloenzyme with zinc at its catalytic center (1, 2, 28). In *Flavobacterium* and *B. diminuta*, the protein has been shown to be membrane associated, and a 29-amino-acid-long signal peptide found in its precursor form has been deduced to be responsible for membrane targeting (24, 25, 36). A similar signal sequence is also encoded in *opd* genes identified in *Agrobacterium radiobacter* (15) and *Sphingomonas* sp. strain JK1 (GenBank accession no. ACD85809). While the conservation of a signal peptide in this group of organophosphate hydrolases has been recognized for some time, its biological role and its precise involvement in the membrane localization of OPH have not been investigated. In this study, we expressed OPH with a C-terminal His tag in *opd*-negative mutants of *B. diminuta* and established a system to differentiate and localize precursor and mature forms of OPH. We have used this system, together with mutagenesis of the signal peptide-encoding region of the *opd* gene, to demonstrate that membrane targeting of OPH is dependent on the twin arginine translocation (Tat) protein secretion pathway, which facilitates localization of OPH to the periplasmic face of the inner membrane.

MATERIALS AND METHODS

Bacterial strains, plasmids, biochemicals, media, and growth conditions. The bacterial strains and plasmids used in the present study are listed in Tables 1 and 2. The wild type and the *opd* mutants of *B. diminuta* were grown in LB medium at 30°C. When necessary, antibiotics ampicillin (100 μg/ml), tetracycline (25 μg/ml), chloramphenicol (30 μg/ml), and polymyxin B (20 μg/ml) were added to the growth medium. Unless otherwise stated, all biochemicals and restriction enzymes were procured either from Sigma Chemicals or from GE Health Care and used following the manufacturer's protocols.

Generation of a *B. diminuta opd* knockout strain. Plasmid pSM3 was digested with PstI, and a 2.1-kb fragment containing *opd*::*tet* was gel extracted and ligated into the PstI site of pSUP202. The resulting plasmid (pSUP*opd*::*tet*) was transformed into *Escherichia coli* S17-1, and this strain was then used as a donor. Conjugation was performed using *B. diminuta* as a recipient by following the procedures described elsewhere (40). The exconjugants were selected by plating the appropriate dilutions of the mating mixture on LB plates containing polymyxin B and tetracycline. The plates were incubated for 48 to 72 h at 30°C, and colonies of *B. diminuta* (*opd*::*tet*) were observed only on plates spread with mating mixture. No colonies were seen on plates spread with either donor or recipient cells. To assess the integration of the *opd*::*tet* cassette into the *opd* gene through homologous recombination, the exconjugants were replica plated on plates having polymyxin B-tetracycline and polymyxin B-chloramphenicol. The colonies that showed resistance to polymyxin B-tetracycline and sensitivity to chloramphenicol were selected for further analysis. Genomic DNA was isolated

* Corresponding author. Mailing address: Dept. of Animal Sciences, School of Life Sciences, University of Hyderabad, Hyderabad 500 046, India. Phone: 91 40 23134578. Fax: 91 40 23010120. E-mail: sdsl@uohyd.ernet.in.

▽ Published ahead of print on 21 August 2009.

TABLE 1. Bacterial strains

Strain	Genotype or phenotype	Source or reference
E. coli DH5α	*supE44* Δ*lacU169* (ϕ80 *lacZ*Δ*M15*) *hsdR17 recA1 endA1 gyrA96 thi-1 relA1*	12
E. coli BL21	*hsdS gal*(λ c*Its*857 *ind1 Sam7 nin5 lacUV5* T7 *gene1*)	42
E. coli S17-1	*thi pro hsdR hsdM recA* RP4 2-Tc::Mu-Km^r::Tn7 (Tp^r Sp^r Sm^r)	40
B. diminuta	Sm^r PmB^r *opd*$^+$	35
B. diminuta opd mutant	Sm^r Tc^r PmB^r *opd*	This work

from the exconjugants that showed sensitivity to chloramphenicol and used to perform PCR using *opd*-specific primers. Similarly, the indigenous plasmids isolated from exconjugants were used to perform Southern hybridization using probes specific for the *opd* and *tet* genes.

Mobilization and expression of plasmids into *B. diminuta*. In our previous studies, we have described cloning of the *opd* gene from *Flavobacterium* sp. strain ATCC 27551 into the broad-host-range expression vector pMMB206 to derive plasmids coding for both the precursor (preOPH) (38) mature (mOPH) forms of OPH, both with a C-terminal His tag (30). As the *opd* genes from *Flavobacterium* sp. strain ATCC27551 and *B. diminuta* are identical (13), expression plasmids pSM5 (encoding preOPH) and pHLNS400 (encoding mOPH) were mobilized into *B. diminuta* by conjugation from *E. coli* S17-1. Overnight cultures of *E. coli* S17-1 containing either pSM5 or pHLNS400 were used as donors and mixed with the similar cultures of *B. diminuta opd*::*tet* mutants at a 3:1 ratio. The cells from this mixture were collected on a 2-μm filter, and filter mating was performed essentially as described elsewhere (34). After mating, exconjugants were selected on tetracycline and chloramphenicol plates and grown at 30°C for 48 h. Successful plasmid transfer was confirmed by PCR using M13 universal forward and reverse primers which amplify the *opd* gene cloned in the expression vector.

Expression and subcellular localization of OPH in *B. diminuta*. Overnight cultures (1 ml) of *B. diminuta* containing expression plasmids were inoculated into 100 ml of LB medium. The culture was grown at 30°C till it reached an optical density at 600 nm of 0.5, and isopropyl-β-D-thiogalactopyranoside (IPTG) was then added to a final concentration of 1 mM to induce the expression of OPH. Cultures were grown for a further period of 2 h, and the expression of OPH was monitored by assaying the enzyme's activity. After confirmation of OPH expression, cells were harvested and resuspended in buffer (0.5 M sucrose, 5 mM EDTA, 50 mM Tris-HCl, pH 8.0) containing 600 μg/ml of lysozyme, and the periplasmic fraction was carefully isolated using standard procedures (44, 45). After the periplasm was separated, the spheroplasts were transferred to a new tube and used for isolation of membrane and cytoplasmic fractions. For membrane fraction isolation, spheroplasts were prepared from 150 ml of induced culture and sonicated on ice (approximately four cycles, each with 40 s of sonication and 30 s of rest) until the suspension was clarified. The lysate was subjected to ultracentrifugation at 48,000 rpm for 1 h, and the supernatant was transferred to a new tube and used as the cytoplasmic fraction. The pellet containing the membrane fraction was dissolved in 1 ml of buffer (10 mM phosphate buffer, pH 7.0) and recentrifuged under the same conditions to remove traces of cytoplasm from membrane preparations. The purity of the cell fractions was established by assaying marker enzymes before they were used for further studies. Acid phosphatase, nitrate reductase, and glucose-6-phosphate dehydrogenase were used as periplasmic, membrane, and cytoplasmic markers, respectively (33). The proteins in these fractions were then analyzed on 12.5% sodium dodecyl sulfate-polyacrylamide gel electrophoresis (SDS-PAGE) gels, and the presence of OPH was monitored by performing Western blot assays using anti-His antibody, followed by enhanced chemiluminescence detection. The precursor and mature forms of OPH in *B. diminuta* were identified by comparing the size of the signals with the signals obtained for the purified recombinant precursor and mature forms of OPH encoded by plasmids pHYS400 (39) and pHNS400 (30), respectively.

OPH variants with changes in the Tat motif. Mutants of *opd* encoding OPH variants in which the invariant arginines of the Tat motif were replaced with amino acids having either similar charge or shape were generated by PCR mutagenesis. Plasmid pPHYS400 was used as template, the forward primer contained the desired mutation, and the T7 terminator primer was used as the reverse primer. PCR was performed using *Pfu* polymerase, and the amplicons were digested with EcoRI and BamHI and cloned in pMMB206. The resultant plasmids and the mutations they carry are listed in Table 1.

Construction of *opd-gfp* fusions. Plasmid pSM5 was used to generate in-frame fusions of *gfp* with the *opd* gene. The *opd* gene contains a SalI site 300 bp downstream of the start codon ATG, and pSM5 has a unique HindIII site in the multiple cloning site of the vector. Hence, digestion with SalI and HindIII removes the 3′ end of the gene. To generate an expression plasmid encoding preOPH-GFP, the *gfp* gene was amplified from pBQGFP using forward (5′ GGA GAT ATG TCG ACG GCT AGC AAA GGA GAA GAA CTC 3′) and reverse (5′ GCT TTG TTA GCA AAG CTT TCC TCA GTT GTA CAG 3′) primers and cloned into the SalI and HindIII sites (underlined) of pSM5 to give pYSGFP400, in which *gfp* is in frame with the 5′ end of *opd* that includes the coding region for the signal peptide of OPH. A similar cloning strategy was followed to introduce the SsrA signal (18, 19) downstream of the green fluorescent protein (GFP)-coding sequences, except that an oligonucleotide (GCAGCAAACGACGAAA

TABLE 2. Plasmids

Plasmid	Relevant description	Source or reference
pBQGFP	Amp^r; *gfp* cloned in pUC18	Gift from J. R. Wild
pCMS1::*tet*	pCMS1 containing an *opd*::*tet* insertion	This work
pHLNS400	Cm^r; *opd* gene encoding mature OPH-6His cloned as an EcoRI-BamHI fragment in pMMB206 under the control of p*tac*	30
pHNS400	Amp^r; *opd* sequence encoding mature OPH cloned in pET23b as an NdeI-XhoI fragment	30
pHYS400	Amp^r; complete *opd* gene encoding preOPH cloned in pET23b as an NdeI-XhoI fragment	39
pMMB206	Cm^r; broad-host-range, low-copy-no. expression vector	23
pNSGFP400	Cm^r; *gfp* fused in-frame to the 5′ end of an *opd* gene encoding mOPH by cloning as a SalI-HindIII fragment in pHLNS400	This work
pNSGFPD400	Cm^r; *gfp-ssrA* fused in-frame to the 5′ end of an *opd* gene encoding mOPH by cloning as a SalI-HindIII fragment in pHLNS400	This work
pPHKK400	Cm^r; derivative of pSM5 encoding OPH R4K R5K	This work
pPHRA400	Cm^r; derivative of pSM5 encoding OPH R5A	This work
pPHRK400	Cm^r; derivative of pSM5 encoding OPH R5K	This work
pPHQQ400	Cm^r; derivative of pSM5 encoding OPH R4Q R5Q	This work
pSM3	Amp^r Tc^r; *tet* gene inserted into *opd* (*opd*::*tet*)	38
pSM5	Cm^r; *opd* gene encoding preOPH-6His cloned as an EcoRI-BamHI fragment in pMMB206 under the control of p*tac*	38
pSUP*opd*::*tet*	Cm^r Tc^r; *opd*::*tet* cloned in pSUP202 as a PstI fragment	This work
pSUP202	Mob$^+$ Amp^r Cm^r Tc^r; mobilizable suicide vector	40
pYSGFP400	Cm^r; *opd-gfp* derived by cloning *gfp* as a SalI-HindIII fragment in pSM5	This work
pYSGFPD400	Cm^r; *opd-gfp-ssrA* derived by cloning *gfp-ssrA* as a SalI-HindIII fragment in pSM5	This work

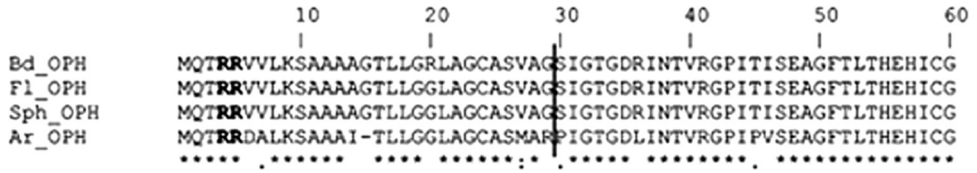

FIG. 1. Presence of Tat motif in OPH signal sequences. Alignment of the N-terminal amino acid sequences of organophosphate hydrolase (OPH) encoded by *opd* genes from *B. diminuta* (Bd), *Flavobacterium* sp. strain ATCC27551 (Fl), *Agrobacterium radiobacter* (Ar), and *Sphingomonas* sp. strain JK1 (Sph). The point of signal sequence cleavage, which has been determined experimentally in *B. diminuta* and *Flavobacterium*, is marked with a vertical line, and the conserved twin-arginine motif is shown in bold type. *, identity; :, similarity; ., weak similarity.

ACTACGCTTTAGCAGCT) with codons that specify amino acids AANDENY ALAA at the C-terminal end of GFP was used as the reverse primer. The plasmid encoding preOPH-GFP with an SsrA signal (preOPH-GFP-SsrA) was designated pYSGFPD400. Comparable plasmids encoding the mature form of OPH (mOPH) were constructed using an identical strategy, except that pHLNS400 was the recipient plasmid. The plasmids coding for mOPH-GFP and mOPH-GFP with an SsrA signal (mOPH-GFP-SsrA) were designated pNSGFP400 and pNSGFPD400, respectively.

Fluorescence-activated cell sorting (FACS) analysis of *opd-gfp* expression. Overnight cultures of *B. diminuta* carrying pYSGFP400, pYSGFPD400, pNS GFP400, or pNSGFPD400 were grown to mid-log phase in LB in the presence of appropriate antibiotics and then induced with 1 mM IPTG for 2 h. Cells were then harvested, extensively washed with phosphate buffer, and resuspended in the same buffer before being analyzed in a BD Pharmingen FACSort. *B. diminuta* wild-type cells served as negative controls. The significance of the relevant comparisons between mean fluorescence values was determined by performing a *t* test.

Treatment of spheroplasts with proteinase K. Spheroplasts prepared from 150-ml cultures of *B. diminuta*(pSM5) were treated with proteinase K (0.5 mg/ml) for 30 min on ice. After incubation, the activity of proteinase K was inhibited by adding phenylmethylsulfonyl fluoride to a final concentration of 1 mM. Subsequently, about 100 μl of spheroplasts was taken from the reaction mixture and carefully added to tubes containing 900 μl of Tris-HCl (pH 8.0) buffer containing 0.75 M sucrose and 100 μmol methyl parathion. OPH activity was measured using previously described procedures (8). Using the remaining portion of the spheroplast preparation, membrane and cytoplasmic fractions were prepared and used to establish the presence of OPH by performing Western blot assays and by assaying OPH activity. Parallel experiments were conducted under identical conditions but omitting proteinase K treatment.

Fluorescence microscopy. A single colony of *B. diminuta* carrying either pYS GFP400 or pYSGFPD400 was inoculated into 3 ml of LB broth with appropriate antibiotics. One percent of an overnight culture was then used to inoculate 10 ml of LB broth, grown to an optical density at 600 nm of 0.5, and induced with 1 mM IPTG at 30°C for 2 h. Cells were harvested at 6,000 rpm for 10 min at 4°C and washed three times in 10% sterile ice-cold glycerol. Cells were then incubated with FM4-64 [*N*-(3-triethylammoniumpropyl)-4-(*p*-diethylaminophenylhexatrienyl)-pyridinium 2Br], a membrane-specific dye (11), for 2 min at room temperature and then fixed on a poly-L-lysine-coated glass slide for confocal microscopic analysis. Confocal microscopy was performed using a Leica confocal laser scanning microscope (Leica Microsystems, Milano, Italy) equipped with argon, krypton, helium, and neon (ARKN) lasers. The fluorescence of GFP was induced with the 488-nm line of the argon laser, and the red fluorescence of FM4-64 with the 543-nm line of the helium neon laser. Corresponding bright-field images were collected through the differential interference contrast channel and detected using the transmission detector of the confocal microscope. Images were processed using the image software supplied by the microscope manufacturer. Contrast and brightness levels were adjusted with Adobe Photoshop 7.0.

RESULTS

The OPH signal peptide contains a twin arginine motif. On examination of the signal sequences of the OPH proteins encoded by *B. diminuta*, *Flavobacterium* sp. strain ATCC27551, *A. radiobacter* P230, and *Sphingomonas* sp. strain JK1, a conserved motif (MQTRRXXLK) was identified (Fig. 1) which has significant resemblance to the consensus sequence (S/T-R-R-X-F-L-K) that typifies Tat-dependent proteins (41). Such proteins are targeted to and exported across the cell membrane using a Sec-independent secretion pathway that is known as the twin arginine transport (Tat) pathway due to the nearly invariant twin arginine dipeptide in the signal sequence (3). The majority of *tat* substrates are periplasmic proteins having a requirement for large cofactors (5). They usually contain multiatom cofactors that are inserted into the protein in the cytoplasm in a manner concomitant with folding such that they are rendered incompatible with the Sec pathway, which exports unfolded substrates (4, 29). Although a number of Tat substrates which lack cofactors have been identified in recent years, the presence of a *tat* signal peptide in an enzyme requiring a simple metal ion cofactor, such as Zn^{2+}, for its catalytic activity is rather unusual. In such cases, cofactor binding usually occurs only after the protein has been transported to the periplasm (5).

The conservation of a potential Tat-dependent signal peptide in OPH proteins suggests that the motif is functionally important, and this prompted us to undertake a detailed study to elucidate its role in membrane targeting of OPH. In order to elucidate the role of the signal peptide in membrane targeting, we chose to use a variant of OPH with a C-terminal His tag (OPH-6His) to facilitate localization of the protein by Western blotting with an anti-His antibody. A genetic background was then required that encoded OPH-6His exclusively, thereby avoiding complications from the presence of wild-type OPH. In the present study, we created a *B. diminuta opd* knockout strain by replacing the wild-type *opd* gene with *opd*::*tet*. Successful homologous recombination was confirmed by PCR using *opd*-specific primers, the amplicon size of *opd*::*tet* being 2.2 kb, compared with 1.2 kb for *opd*. The indigenous plasmid pCMS1, on which the *B. diminuta opd* gene is located, was isolated from these strains, and Southern hybridization was performed after restriction with PstI, using radiolabeled *opd* and *tet* sequences as probes. Detection of a 2.2-kb PstI fragment by both probes (data not shown) confirmed the integration of *opd*::*tet* into the plasmid, which was designated pCMS1::*tet*. As predicted, a *B. diminuta* strain carrying pCMS1::*tet* was OPH negative.

Expression and localization of OPH in *B. diminuta*. Plasmids encoding the wild-type *opd* gene or its variants were mobilized into *B. diminuta*(pCMS1::*tet*), and their expression was induced with IPTG. The expression of OPH was assessed both by measuring the enzyme activity and by Western blotting following separation of proteins by SDS-PAGE. Both the preOPH and mOPH forms were detected in whole-cell extracts from cells carrying pSM5 (Fig. 2A, lane 3). In order to localize OPH, cells were fractionated into cytoplasm, periplasm, and mem-

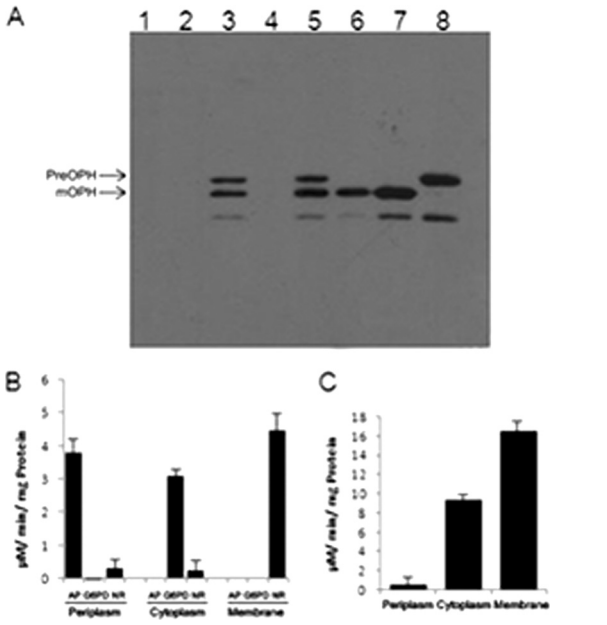

FIG. 2. Expression and subcellular localization of OPH. (A) Western blot (using anti-His antibody) to detect OPH-6His in SDS-PAGE of total cellular proteins of *B. diminuta* (*opd*::*tet*) without (lane 2) and with (lane 3) expression plasmid pSM5. Lanes 4, 5, and 6, periplasmic, cytoplasmic, and membrane fractions from induced cultures of *B. diminuta*(pSM5). Lanes 7 and 8, purified recombinant mOPH and preOPH proteins expressed from *E. coli* BL21 cells. Lane 1, molecular weight markers. (B) Assay of marker enzymes acid phosphatase (AP), glucose-6 phosphate dehydrogenase (G6PD), and nitrate reductase (NR) in periplasmic, cytoplasmic, and membrane fractions. Enzyme activities are given as μmoles of product formed per minute per mg of protein. (C) OPH activity (μmoles of *p*-nitrophenol formed per minute per mg of protein) in periplasmic, cytoplasmic, and membrane fractions. Bars shows results of three independent experiments. Error bars show standard deviations.

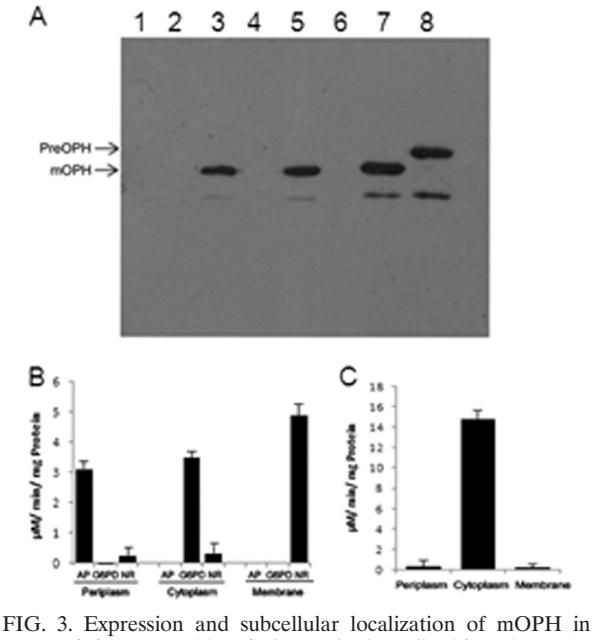

FIG. 3. Expression and subcellular localization of mOPH in *B. diminuta*. (A) Western blots (using anti-His antibody) to detect OPH-6His in SDS-PAGE of total cellular proteins of *B. diminuta* without (lane 2) and with (lane 3) expression plasmid pHLNS400. Lanes 4, 5, and 6, periplasmic, cytoplasmic, and membrane fractions from induced cultures of *B. diminuta*(pHLNS400). Lanes 7 and 8, pure mOPH and preOPH used as markers. Lane 1, molecular weight markers. (B) Assay of marker enzymes acid phosphatase (AP), glucose-6 phosphate dehydrogenase (G6PD), and nitrate reductase (NR) in periplasmic, cytoplasmic, and membrane fractions. Enzyme activities are given as μmoles of product formed per minute per mg of protein. (C) OPH activity (μmoles of *p*-nitrophenol formed per minute) per mg of protein in periplasmic, cytoplasmic, and membrane fractions. Bars shows results of these independent experiments. Error bars show standard deviations.

brane fractions, and the effectiveness of this fractionation was confirmed by measuring the activities of marker enzymes (Fig. 2B). Subsequent analysis of subcellular fractions showed that preOPH was only present in the cytoplasmic fraction, while mOPH was present in both the cytoplasmic and membrane fractions (Fig. 2A, lanes 5 and 6). Neither preOPH nor mOPH was found free in the periplasm (Fig. 2A, lane 4), confirming that OPH is a membrane-associated protein and is not exported into the periplasm. The detection of considerable amounts of mOPH in the cytoplasm was not expected, and we consider that this may be due to the presence of excess OPH in the cells as a consequence of induction of *opd* gene expression from the *lac* promoter of pMMB206. Such overexpression may saturate the Tat machinery such that the signal peptide can be cleaved from OPH but all of the processed enzyme cannot be translocated across the membrane (46). After demonstrating the membrane association of OPH, we attempted to examine whether OPH gains its folded conformation while it is still in the cytoplasm. We expressed mOPH from pHLNS400 in the *opd*-negative mutant of *B. diminuta*, assuming that OPH activity will be detected only when it acquires a native conformation due to proper folding and insertion of cofactor. Protein extracts prepared from these cells had a greater activity than that found in the cellular extracts prepared from the cells coding for preOPH (Fig. 3C). Cells were fractionated, and the purity of the fractions was assessed again using marker enzymes (Fig. 3B). Western blots of subcellular fractions confirmed the presence of mOPH only in the cytoplasm (Fig. 3A, lane 5), with no signal in either the periplasm (Fig. 3A, lane 4) or the membrane (Fig. 3A, lane 6), suggesting that the signal peptide is required only for membrane targeting and not for proper folding and activity of OPH.

OPH is a Tat substrate. In order to examine the hypothesis that *B. diminuta* OPH is a Tat pathway substrate, we examined the effects of replacing one or both of the two arginine residues within the signal peptide. These residues are usually absolutely necessary for the correct recognition and processing of Tat substrates by the Tat translocation machinery. Studies using other systems have determined that the first arginine of the Arg-Arg dipeptide can be replaced with Lys and the second arginine can be replaced with Gln or Asn, as well as Lys, but the replacement of both Arg residues with Lys blocks the export of Tat substrate proteins (7, 9, 16, 41). We generated four variants of the OPH signal peptide based on plasmid pSM5. These variants (R5A, R5K, R4K R5K, and R4Q R5Q) were then analyzed by Western blotting of total cell extracts and subcellular fractions in order to determine whether the

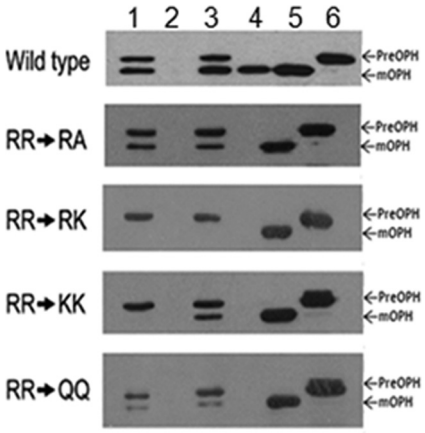

FIG. 4. Western blots of protein extracts from *B. diminuta* cells expressing OPH variants with amino acid substitutions in the invariant arginines of the *tat* motif. The nature of the substitutions is shown alongside each panel. Lane 1, total cellular proteins. Lanes 2, 3, and 4, protein extracts from periplasmic, cytoplasmic, and membrane fractions. Lanes 5 and 6, pure mOPH and preOPH.

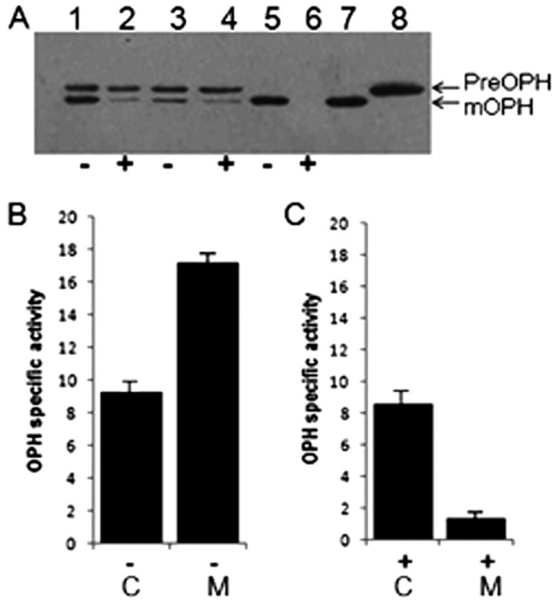

FIG. 5. Localization of OPH by proteinase K treatment of spheroplasts. (A) Western blots (using anti-His_6 antibody) of *B. diminuta*(pSM5). Lanes 1 and 2, spheroplasts; lanes 3 and 4, cytoplasmic fraction from spheroplasts; lanes 5 and 6, membrane fraction from spheroplasts. Lanes 1, 3, and 5, without proteinase K (−); lanes 2, 4, and 6, after proteinase K treatment (+). Lane 7, *E. coli* BL21(pHNS400), expressing mOPH; lane 8, *E. coli* BL21(pHYS400), expressing preOPH. (B) OPH activity (μmoles of *p*-nitrophenol produced per minute per mg of protein) of cytoplasmic (C) and membrane (M) fractions from spheroplasts of *B. diminuta*(pSM5) before proteinase K treatment. (C) Represents activities as described for panel B after proteinase K treatment.

signal peptide was correctly cleaved and whether the mature protein was targeted to the cell membrane.

The data in Fig. 4 strongly support the proposition that the RR dipeptide is crucial for efficient transport and subsequent targeting of OPH to the membrane. None of the OPH variants having substitutions for one or both arginines was found in the membrane fraction. While certain variants showed a small degree of processing, the R5K variant showed the strongest phenotype and remained completely unprocessed. However, even in those variants that showed some processing, none of the processed OPH was apparently subsequently correctly targeted to the membrane. Given that signal peptide processing occurs at the periplasmic side of the cytoplasmic membrane, the protein must have been correctly targeted to the membrane, and it would therefore appear that for these OPH variants, the processed form is not stably associated with the membrane. Nevertheless, the properties of these four variants clearly confirm the essential nature of the Arg-Arg dipeptide within the OPH signal sequence and are consistent with OPH being a Tat substrate.

OPH localization on the membrane. Our experimental evidence clearly indicates that OPH is processed in a *tat*-dependent manner. However, unlike most Tat substrates, it is apparently not exported to the periplasm but, rather, is found to be tightly membrane associated. We therefore wished to establish on which face of the membrane the mature OPH was located. To do this, we prepared spheroplasts of *B. diminuta*(pSM5) and examined the effect both on OPH localization and activity of treating them with proteinase K. We used Western blotting to detect both preOPH and mOPH in whole spheroplasts before and after proteinase K treatment and, similarly, in cytoplasmic and membrane fractions prepared from these spheroplasts (Fig. 5A). Proteinase K very significantly reduced the levels of mOPH detected in the spheroplasts, and cell fractionation showed that membrane-associated mOPH was completely removed by proteinase K treatment. This was supported by the almost complete loss of membrane-associated OPH activity from the membrane fraction following treatment with proteinase K (Fig. 5B and C). These data demonstrate definitively that mOPH is located on the periplasmic face of the inner cell membrane.

In order to reinforce these results, we constructed *opd-gfp* fusions encoding pfOPH-GFP with and without an SsrA-coding sequence at the 3′ end of *gfp* and expressed them in *B. diminuta*. Though GFP, when fused to the appropriate signal peptide, is capable of translocating across the membrane via Sec and Tat pathways, the periplasmic environment is not favorable for GFP to acquire the folded confirmation needed to emit fluorescence (10). Consequently, GFP only retains fluorescence when translocated to the periplasm via the Tat pathway (32, 43). Proteins with an SsrA signal at their C terminus are identified as incompletely translated proteins and driven to the intracellular proteolytic ClpXP machinery for degradation (19). Hence, if preOPH-GFP is located on the periplasmic face, it would escape proteolytic degradation despite having an SsrA signal at the C terminus and would retain the ability to show fluorescence.

B. diminuta strains carrying plasmids pYSGFP400, pYSG FPD400, pNSGFP400, and pNSGFPD400 were induced for OPH-GFP expression and then subjected to FACS and Western analysis as described in Materials and Methods. The mean fluorescence values obtained for cells expressing preOPH-GFP (20.19) and preOPH-GFP-SsrA (20.15) were not significantly different ($t = 0.84$, $P > 0.1$), indicating that preOPH-GFP-SsrA was not accessible to the intracellular proteolytic ClpXP machinery and had been translocated across the inner mem-

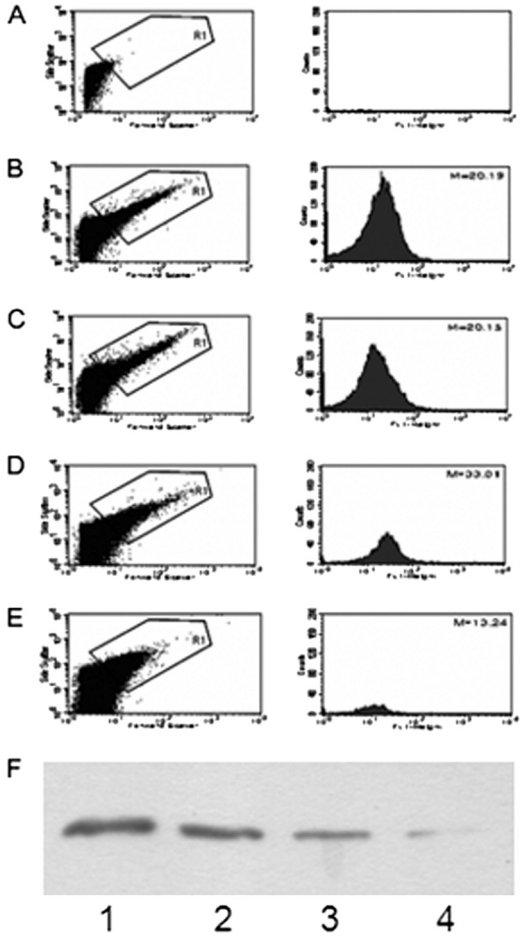

FIG. 6. FACS analysis of OPH localization using OPH-GFP. Left column, dot plots of raw data. The polygon in each graph identifies the gate R1 used for generation of histograms. Right column, histograms of counts from gate R1 for each strain. M = 20.19, 20.15, 33.01, and 13.24 for panels B through E, respectively. (A) Wild-type *B. diminuta* cells. (B to D) *B. diminuta* cells expressing preOPH-GFP (B), preOPH-GFP-SsrA (C), mOPH-GFP (D), and mOPH-GFP-SsrA (E). (F) Presence of OPH-GFP fusion proteins in *B. diminuta* cells having expression plasmids coding for preOPH-GFP (lane 1), preOPH-GFP-SsrA (lane 2), mOPH-GFP (lane 3), and mOPH-GFP-SsrA (lane 4). Total cell proteins from the respective cultures were analyzed by SDS-PAGE, and Western blots were performed using anti-GFP antibodies.

brane (Fig. 6B and C). Consistent with this, when the proteins were expressed in the cytoplasm as a consequence of removing the signal peptide, i.e., using mOPH-GFP, the presence of the SsrA signal very significantly reduced the mean fluorescence ($t = 54.04, P < 0.001$) (Fig. 6D and E). The levels of expression of the OPH-GFP fusion proteins were determined by Western blotting, which confirmed that the presence of the SsrA signal selectively eliminated mOPH-GFP (Fig. 6F, lane 4) while showing no significant effect on pre-OPH-GFP (Fig. 6F, lane 2). Since the GFP fusions to both preOPH and mOPH retained fluorescence, this clearly indicates that the GFP is folded before transport and would require export by the Tat system. Fluorescence microscopy of cells expressing preOPH-GFP and stained with the membrane-specific dye FM4-64 reinforced this conclusion, as it showed GFP-dependent fluorescence surrounding the inner membrane (Fig. 7).

DISCUSSION

Early studies of organophosphate hydrolase (OPH) identified its apparent membrane association by performing cell fractionation and ultracentrifugation studies (22, 25). Subsequent cloning and sequencing of the *opd* gene, together with N-terminal sequencing of purified OPH, indicated the presence of a signal peptide (24). However, the precise nature of that signal peptide and its relationship to the membrane localization of OPH has remained unexplored until now.

In this study, we have shown that the OPH signal peptide has the characteristic twin arginine motif found in nearly all proteins that are subject to membrane translocation by the Tat system. Furthermore, in vivo experiments with *B. diminuta* support the proposition that OPH is a Tat substrate. Tat substrates are typically folded prior to translocation from the cytoplasm, and this is the case for OPH, which is fully active in the cytoplasm if the signal peptide is removed such that it cannot be translocated. Previous attempts to express OPH in *E. coli* have not been very successful, with most activity being retained in the soluble fraction and not membrane associated, and expression levels were improved when the signal peptide sequence was deleted and the mature protein was expressed in the cytoplasm (24, 36). These results suggest some incompatibility between the native Tat signal peptide and the *E. coli* Tat system. A study in 2005 reported the fusing of the OPH gene to the Tat signal sequence of the *E. coli* TMAO reductase (TorA) protein to facilitate OPH secretion to the periplasm (17). In order to make this construct, the authors deleted the native signal sequence but apparently did not recognize that it already encodes a Tat signal peptide.

A number of types of proteins have been shown to utilize the Tat system (21). These include proteins containing multiatom cofactors, for which synthesis, maturation, and incorporation of the cofactor takes place in the cytoplasm; proteins containing simple metal ion cofactors that normally bind the cofactor after transport to the periplasm; multimeric proteins that assemble with partner subunits before transport; proteins that fold rapidly after translation; and proteins for which the periplasmic environment is unfavorable for folding and which are translocated by the Tat pathway to escape from DegP-mediated degradation (31). While OPH requires the presence of zinc at its catalytic center, this should not necessarily require it to be folded prior to translocation. However, the periplasmic amidases of *E. coli*, AmiA and AmiC, are also Tat substrates and have been suggested to be zinc enzymes. Furthermore, AmiA, like OPH, is tightly bound to the periplasmic face of the inner membrane, though it can be released by 250 mM NaCl (6). We have previously described a metafission hydrolase (MfhA) which is encoded by the *mfhA* gene located adjacent to the *opd* gene on the pPDL2 plasmid of *Flavobacterium* sp. strain ATCC27551 (20), and our recent studies indicate that MfhA can form a complex with OPH. Given that MfhA has no signal peptide, it is possible that it could be cotranslocated with OPH to produce an active complex on the periplasmic face of the inner membrane and that such cotranslocation would require Tat dependency.

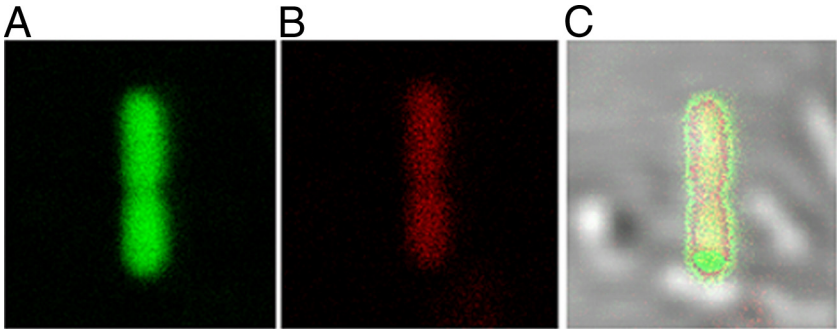

FIG. 7. Fluorescence microscopy localization of preOPH-GFP. (A) Fluorescence microscopic image of *B. diminuta* cells expressing preOPH-GFP. (B) Image taken after staining the cells with the membrane-specific dye FM4-64. (C) Overlay of images shown in panels A and B.

Questions that remain following these studies are why OPH should be located in the periplasm rather than the cytoplasm and what mechanism facilitates its tight membrane association. As already mentioned, OPH can function effectively in the cytoplasm and, indeed, engineering of *B. diminuta* OPH to facilitate expression in *E. coli* has been achieved by removal of the signal peptide so as to force cytoplasmic synthesis of active enzyme (36). So it is not immediately apparent why OPH should undergo membrane translocation. Likewise, there are some examples of proteins that are translocated by the Tat system and subsequently anchored to the membrane on its periplasmic face, and these include some hydrogenases that are membrane anchored by a single C-terminal transmembrane helix (14). However, OPH has no potential transmembrane helix (1), and so it must use some other, possibly novel, mechanism to facilitate membrane association.

ACKNOWLEDGMENTS

B. diminuta used in this study was obtained from Jim Wild's laboratory. We would like to thank Tracy Palmer for helpful advice.

P.G. was the recipient of a Rajiv Gandhi National Junior Research Fellowship. S.P. was the recipient of a Shantha Excellence Junior Research Fellowship. Research in the laboratory of D.S. is supported by DST, DBT, CSIR, and DRDO. M.M. acknowledges support from the Biotechnology and Biological Sciences Research Council (United Kingdom). The School of Life Sciences, University of Hyderabad, is funded by DBT (CREBB), DST (FIST), and UGC (CAS).

REFERENCES

1. **Benning, M. M., J. M. Kuo, F. M. Raushel, and H. M. Holden.** 1994. Three-dimensional structure of phosphotriesterase: an enzyme capable of detoxifying organophosphate nerve agents. Biochemistry **33:**15001–15007.
2. **Benning, M. M., J. M. Kuo, F. M. Raushel, and H. M. Holden.** 1995. Three-dimensional structure of the binuclear metal center of phosphotriesterase. Biochemistry **34:**7973–7978.
3. **Berks, B. C.** 1996. A common export pathway for proteins binding complex redox cofactors? Mol. Microbiol. **22:**393–404.
4. **Berks, B. C., T. Palmer, and F. Sargent.** 2003. The Tat protein translocation pathway and its role in microbial physiology. Adv. Microb. Physiol. **47:**187–254.
5. **Berks, B. C., T. Palmer, and F. Sargent.** 2005. Protein targeting by the bacterial twin-arginine translocation (Tat) pathway. Curr. Opin. Microbiol. **8:**174–181.
6. **Bernhardt, T. G., and P. A. de Boer.** 2003. The *Escherichia coli* amidase AmiC is a periplasmic septal ring component exported via the twin-arginine transport pathway. Mol. Microbiol. **48:**1171–1182.
7. **Buchanan, G., F. Sargent, B. C. Berks, and T. Palmer.** 2001. A genetic screen for suppressors of *Escherichia coli* Tat signal peptide mutations establishes a critical role for the second arginine within the twin-arginine motif. Arch. Microbiol. **177:**107–112.
8. **Chaudhry, G. R., A. N. Ali, and W. B. Wheeler.** 1988. Isolation of a methyl parathion-degrading *Pseudomonas* sp. that possesses DNA homologous to the *opd* gene from a *Flavobacterium* sp. Appl. Environ. Microbiol. **54:**288–293.
9. **DeLisa, M. P., P. Samuelson, T. Palmer, and G. Georgiou.** 2002. Genetic analysis of the twin arginine translocator secretion pathway in bacteria. J. Biol. Chem. **277:**29825–29831.
10. **Feilmeier, B. J., G. Iseminger, D. Schroeder, H. Webber, and G. J. Phillips.** 2000. Green fluorescent protein functions as a reporter for protein localization in *Escherichia coli*. J. Bacteriol. **182:**4068–4076.
11. **Fischer-Parton, S., R. M. Parton, P. C. Hickey, J. Dijksterhuis, H. A. Atkinson, and N. D. Read.** 2000. Confocal microscopy of FM4-64 as a tool for analysing endocytosis and vesicle trafficking in living fungal hyphae. J. Microsc. **198:**246–259.
12. **Hanahan, D.** 1983. Studies on transformation of *Escherichia coli* with plasmids. J. Mol. Biol. **166:**557–580.
13. **Harper, L. L., C. S. Mcdaniel, C. E. Miller, and J. R. Wild.** 1988. Dissimilar plasmids isolated from *Pseudomonas diminuta* MG and a *Flavobacterium* sp. (ATCC 27551) contain identical *opd* genes. Appl. Environ. Microbiol. **54:**2586–2589.
14. **Hatzixanthis, K., T. Palmer, and F. Sargent.** 2003. A subset of bacterial inner membrane proteins integrated by the twin-arginine translocase. Mol. Microbiol. **49:**1377–1390.
15. **Horne, I., T. D. Sutherland, R. L. Harcourt, R. J. Russell, and J. G. Oakeshott.** 2002. Identification of an *opd* (organophosphate degradation) gene in an *Agrobacterium* isolate. Appl. Environ. Microbiol. **68:**3371–3376.
16. **Ize, B., F. Gerard, and L. F. Wu.** 2002. *In vivo* assessment of the Tat signal peptide specificity in *Escherichia coli*. Arch. Microbiol. **178:**548–553.
17. **Kang, D. G., G. B. Lim, and H. J. Cha.** 2005. Functional periplasmic secretion of organophosphorous hydrolase using the twin-arginine translocation pathway in *Escherichia coli*. J. Biotechnol. **118:**379–385.
18. **Karzai, A. W., E. D. Roche, and R. T. Sauer.** 2000. The SsrA-SmpB system for protein tagging, directed degradation and ribosome rescue. Nat. Struct. Biol. **7:**449–455.
19. **Keiler, K. C., P. R. Waller, and R. T. Sauer.** 1996. Role of a peptide tagging system in degradation of proteins synthesized from damaged messenger RNA. Science **271:**990–993.
20. **Khajamohiddin, S., P. S. Babu, D. Chakka, M. Merrick, A. Bhaduri, R. Sowdhamini, and D. Siddavattam.** 2006. A novel meta-cleavage product hydrolase from *Flavobacterium* sp. ATCC27551. Biochem. Biophys. Res. Commun. **351:**675–681.
21. **Lee, P. A., D. Tullman-Ercek, and G. Georgiou.** 2006. The bacterial twin-arginine translocation pathway. Annu. Rev. Microbiol. **60:**373–395.
22. **McDaniel, C. S., L. L. Harper, and J. R. Wild.** 1988. Cloning and sequencing of a plasmid-borne gene (*opd*) encoding a phosphotriesterase. J. Bacteriol. **170:**2306–2311.
23. **Morales, V. M., A. Backman, and M. Bagdasarian.** 1991. A series of wide-host-range low-copy-number vectors that allow direct screening for recombinants. Gene **97:**39–47.
24. **Mulbry, W. W., and J. S. Karns.** 1989. Parathion hydrolase specified by the *Flavobacterium opd* gene: relationship between the gene and protein. J. Bacteriol. **171:**6740–6746.
25. **Mulbry, W. W., and J. S. Karns.** 1989. Purification and characterization of three parathion hydrolases from gram-negative bacterial strains. Appl. Environ. Microbiol. **55:**289–293.
26. **Mulbry, W. W., J. S. Karns, P. C. Kearney, J. O. Nelson, C. S. McDaniel, and J. R. Wild.** 1986. Identification of a plasmid-borne parathion hydrolase gene from *Flavobacterium* sp. by Southern hybridization with *opd* from *Pseudomonas diminuta*. Appl. Environ. Microbiol. **51:**926–930.
27. **Mulbry, W. W., P. C. Kearney, J. O. Nelson, and J. S. Karns.** 1987. Physical comparison of parathion hydrolase plasmids from *Pseudomonas diminuta* and *Flavobacterium* sp. Plasmid **18:**173–177.
28. **Omburo, G. A., J. M. Kuo, L. S. Mullins, and F. M. Raushel.** 1992. Characterization of the zinc binding site of bacterial phosphotriesterase. J. Biol. Chem. **267:**13278–13283.

29. **Palmer, T., F. Sargent, and B. C. Berks.** 2005. Export of complex cofactor-containing proteins by the bacterial Tat pathway. Trends Microbiol. **13:**175–180.
30. **Pandey, J. P., P. Gorla, B. Manavathi, and D. Siddavattam.** 2009. mRNA secondary structure modulates the translation of organophosphate hydrolase (OPH) in *E. coli*. Mol. Biol. Rep. **36:**449–454.
31. **Ruiz, N., and T. J. Silhavy.** 2005. Sensing external stress: watchdogs of the *Escherichia coli* cell envelope. Curr. Opin. Microbiol. **8:**122–126.
32. **Santini, C. L., A. Bernadac, M. Zhang, A. Chanal, B. Ize, C. Blanco, and L. F. Wu.** 2001. Translocation of jellyfish green fluorescent protein via the Tat system of *Escherichia coli* and change of its periplasmic localization in response to osmotic up-shock. J. Biol. Chem. **276:**8159–8164.
33. **Sargent, F., E. G. Bogsch, N. R. Stanley, M. Wexler, C. Robinson, B. C. Berks, and T. Palmer.** 1998. Overlapping functions of components of a bacterial Sec-independent protein export pathway. EMBO J. **17:**3640–3650.
34. **Sasaki, Y., N. Taketomo, and T. Sasaki.** 1988. Factors affecting transfer frequency of pAMβ1 from *Streptococcus faecalis* to *Lactobacillus plantarum*. J. Bacteriol. **170:**5939–5942.
35. **Segers, P., M. Vancanneyt, B. Pot, U. Torck, B. Hoste, D. Dewettinck, E. Falsen, K. Kersters, and P. De Vos.** 1994. Classification of *Pseudomonas diminuta* Leifson and Hugh 1954 and *Pseudomonas vesicularis* Busing, Doll, and Freytag 1953 in *Brevundimonas* gen. nov. as *Brevundimonas diminuta* comb. nov. and *Brevundimonas vesicularis* comb. nov., respectively. Int. J. Syst. Bacteriol. **44:**499–510.
36. **Serdar, C. M., D. C. Murdock, and M. F. Rohde.** 1989. Parathion hydrolase gene from *Pseudomonas diminuta* MG: subcloning, complete nucleotide-sequence, and expression of the mature portion of the enzyme in *Escherichia coli*. Bio/Technology **7:**1151–1155.
37. **Sethunathan, N., and T. Yoshida.** 1973. A *Flavobacterium* sp. that degrades diazinon and parathion. Can. J. Microbiol. **19:**873–875.
38. **Siddavattam, D., S. Khajamohiddin, B. Manavathi, S. B. Pakala, and M. Merrick.** 2003. Transposon-like organization of the plasmid-borne organophosphate degradation (*opd*) gene cluster found in *Flavobacterium* sp. Appl. Environ. Microbiol. **69:**2533–2539.
39. **Siddavattam, D., E. R. Raju, P. V. E. Paul, and M. Merrick.** 2006. Overexpression of parathion hydrolase in *Escherichia coli* stimulates the synthesis of outer membrane porin OmpF. Pesticide Biochem. Physiol. **86:**146–150.
40. **Simon, R., U. Priefer, and A. Puhler.** 1983. A broad host range mobilization system for in vivo genetic engineering: transposon mutagenesis in Gram-negative bacteria. Bio/Technology. **1:**784–791.
41. **Stanley, N. R., T. Palmer, and B. C. Berks.** 2000. The twin arginine consensus motif of Tat signal peptides is involved in Sec-independent protein targeting in *Escherichia coli*. J. Biol. Chem. **275:**11591–11596.
42. **Studier, F. W., and B. A. Moffatt.** 1986. Use of bacteriophage T7 RNA polymerase to direct selective high-level expression of cloned genes. J. Mol. Biol. **189:**113–130.
43. **Thomas, J. D., R. A. Daniel, J. Errington, and C. Robinson.** 2001. Export of active green fluorescent protein to the periplasm by the twin-arginine translocase (Tat) pathway in Escherichia coli. Mol. Microbiol. **39:**47–53.
44. **van Geest, M., and J. S. Lolkema.** 1996. Membrane topology of the sodium ion-dependent citrate carrier of *Klebsiella pneumoniae*. Evidence for a new structural class of secondary transporters. J. Biol. Chem. **271:**25582–25589.
45. **Weiner, J. H., P. T. Bilous, G. M. Shaw, S. P. Lubitz, L. Frost, G. H. Thomas, J. A. Cole, and R. J. Turner.** 1998. A novel and ubiquitous system for membrane targeting and secretion of cofactor-containing proteins. Cell **93:** 93–101.
46. **Yahr, T. L., and W. T. Wickner.** 2001. Functional reconstitution of bacterial Tat translocation *in vitro*. EMBO J. **20:**2472–2479.